ENERGY AND SEDIMENT BUDGETS OF THE GLOBAL COASTAL ZONE

Douglas L. Inman
Coastal Morphology Group
Integrative Oceanography Division
Scripps Institution of Oceanography
dinman@ucsd.edu

Scott A. Jenkins
Coastal Morphology Group
Integrative Oceanography Division
Scripps Institution of Oceanography
sjenkins@ucsd.edu

20 June 2003

Preprint from *Encyclopedia of Coastal Science* (M. Schwartz, editor),
The Earth Sciences Encyclopedia Online <www.eseo.com>,
with permission from Kluwer Academic Publishers, Dordrecht, The Netherlands.

ENERGY AND SEDIMENT BUDGETS OF THE GLOBAL COASTAL ZONE

The energy for the global coastal zone is primarily powered by solar irradiance and tides. The solar irradiance warms the earth's surface unevenly, driving wind and current systems that redistribute heat and generate storms with rainfall and snow that erode landmasses. The erosion products of sediment and dissolved solids are carried to the sea by rivers and glaciers. Winds, waves, tides, and currents transport and redistribute sediment and sculpt coastal landforms.

Solar irradiance provides an energy flux of about 1.8×10^{14} kilowatt (kW) to the earth. About 2.5×10^{9} kW of mechanical energy in wind-generated waves is incident on the world's 440,000 km coastlines. Another 2.2×10^{9} kW of tidal energy is expended in shallow seas. The total flux of mechanical energy of all kinds in shallow waters of the coastal zone is about 5.5×10^{9} kW. Some of this energy is expended in coastal erosion and transport of the erosion products from the land, and the remainder drives frictional processes and is dissipated as heat. The erosion rate of land is about 6 cm/thousand years resulting in a flux to the sea of 5×10^{9} ton/yr dissolved solids and 20×10^{9} ton/yr particulate solids (1 ton = 1000 kg).

Introduction

The oceans respond to many different kinds of steady and impulsive forces applied at their boundaries with the atmosphere and sea floor. Although most energy in the nearshore waters comes from wind-generated waves and tidal currents, energy

from a number of other sources such as internal waves and ocean currents may also be important locally.

One approach to understanding the relative importance of nearshore processes is to compare the sea's potential to erode the land with the land's potential to supply terrestrial erosion products. Such a comparison ultimately resolves itself into the balance between the budget of power in waves and currents and the budget of sediments available for transport. Of course, this balance varies widely from place to place, and even in the best studied areas is but poorly understood. However, order of magnitude estimates can be attempted on a world-wide basis, and their consideration here gives some overall perspective for the relative importance of the driving forces that are operative in nearshore waters.

In a practical sense, the waters of the coastal zone can be considered as including the shallow seas and the waters covering the continental shelves of the world, an area of 29×10^6 km^2, or about 5.5% of the surface area of the world and about 8% of the area of the world oceans (Table 1). The nearshore waters are bounded on the landward side by coastlines that total about 440,000 km in length, and to the seaward by the break in slope at the shelf edge (shelf break) marking the change from the relatively horizontal continental shelf to the steeper continental slope. The continental slopes are one of the striking geographic features of the earth and have a combined length of about 150,000 km.

Conventionally, the depth of the shelf break is taken as 200 m or 100 fathom, although in some localities the depth may be as great as 400 m. On a world wide basis, the average depth of the shelf break is about 130 m. The width of the shelf ranges from zero to over 1300 km and averages about 74 km (Shepard, 1963). Although having little geomorphic basis, international law defines *territorial seas*

Table 1. Dimensions of major topographic features.

Feature	Area 10^6 km^2	Length of Coastline 10^3 km
Continents	138.8	210.
Large Islands (larger than 2500 km^2)	9.3	136.
Small Islands (25 to 2500 km^2)	0.9	94.
Total Land	149.0 [a]	440.
		Length of Shelf Break 10^3 km
Oceans (depths > 200 m)	332.1	
Continental Shelf (0-200 m)	29.0	149.
Total Marine Water	361.1	
Total Area Earth	510.0	

Source: Inman and Nordstrom (1971) for features with length scales greater than 10 km.

a United Nations (UNEP, 1987) gives total land area of 145 x 10^6 km^2.

as usually extending seaward 12 nautical miles (22.2 km) beyond the coastline and an *Exclusive Economic Zone* as usually extending 200 nautical miles (371 km) seaward.

Budget of energy in shallow water

The current systems of the world's atmosphere and ocean are solar powered. The sun irradiates the earth with a total of about 1.8×10^{14} kilowatts (kW), or an intensity of 1.37 kW/m^2, the so-called solar constant. In terms of the rotating, spherical earth, this averages to about 342 W/m^2 of earth's surface. Of this amount about 30% is reflected and backscattered, 19% is absorbed by the atmosphere, and 51% is absorbed at the earth's surface (e.g., Gill, 1982). Solar energy heats the earth's surface unevenly and generates winds. The oceans are relatively opaque to solar irradiance, so that the effect on the oceans is to stratify and stabilize the surface water. As a consequence the ocean responds much more to wind, even though the intensity of thermal energy from the sun greatly exceeds the mechanical energy from the wind at the water's surface. Averaged over the earth's surface, the intensity of thermal energy absorbed is about 175 W/m^2, while the sea surface stresses and pressures caused by a wind blowing 10 m/s expend about 1.3 W/m^2. In contrast, the mean heat flow to the earth's surface from the interior is approximately 0.1 W/m^2, and occurs mostly at the mid-ocean spreading centers (Pollack *et al.,* 1993). Thus it is the solar powered atmosphere and ocean currents together that maintain the earth's heat budget by accounting for a poleward transport of energy at the rate of about 8×10^9 kW.

Studies of the energy budgets of the ocean and atmosphere (e.g., Webster, 1994) show that the total energy content of the oceans ($\sim 160 \times 10^{25}$ joule (J)) is 1000 times larger than that of the atmosphere ($\sim 125 \times 10^{22}$ J). Because of greater

mass and heat capacity, the oceans play a critical role in controlling and moderating weather and climate. However, in terms of the kinetic energy available for interacting with the oceans, the atmospheric kinetic energy ($\sim 6 \times 10^{20}$ J) is 200 times larger than that of the oceans.

The wind systems are the direct link between atmosphere and ocean and, through momentum exchange at the ocean's surface, expend kinetic energy at the rate of about 10^{11} kW (Malkus, 1962; Newell *et al.,* 1992). The prevailing wind systems cause all large bodies of water to have windward and leeward shores. The Pacific coasts of the Americas are in general windward coasts while the Atlantic seaboards are leeward coasts. The general wind flow is clockwise in the northern hemisphere around semi-permanent, midlatitude areas of high pressure, e.g., the north Pacific high and the Bermuda high in the Atlantic Ocean. Circulation patterns in the southern oceans are essentially counterclockwise flowing mirror images of those in the northern hemisphere (Figure 1).

Sea and swell

The most intense wave action in all oceans results from cyclogenesis over the poleward-flowing, western boundary currents. These warm water jets carry equatorial heat to higher latitudes and produce strong temperature gradients that spin-up intense storms (Figure l). These boundary cyclonic events generate large, high frequency *sea waves* along leeward shores and long waves that cross the ocean and appear as low frequency *swell* on windward coasts. In the north Pacific, dry Siberian winds flowing over the warmer Kuroshio current produce a series of cyclonic cold fronts that collectively have long fetches and generate the high waves for the Pacific coast of North America during the winter. These storms produce swell when they are distant and seawaves as their tracks near the coast.

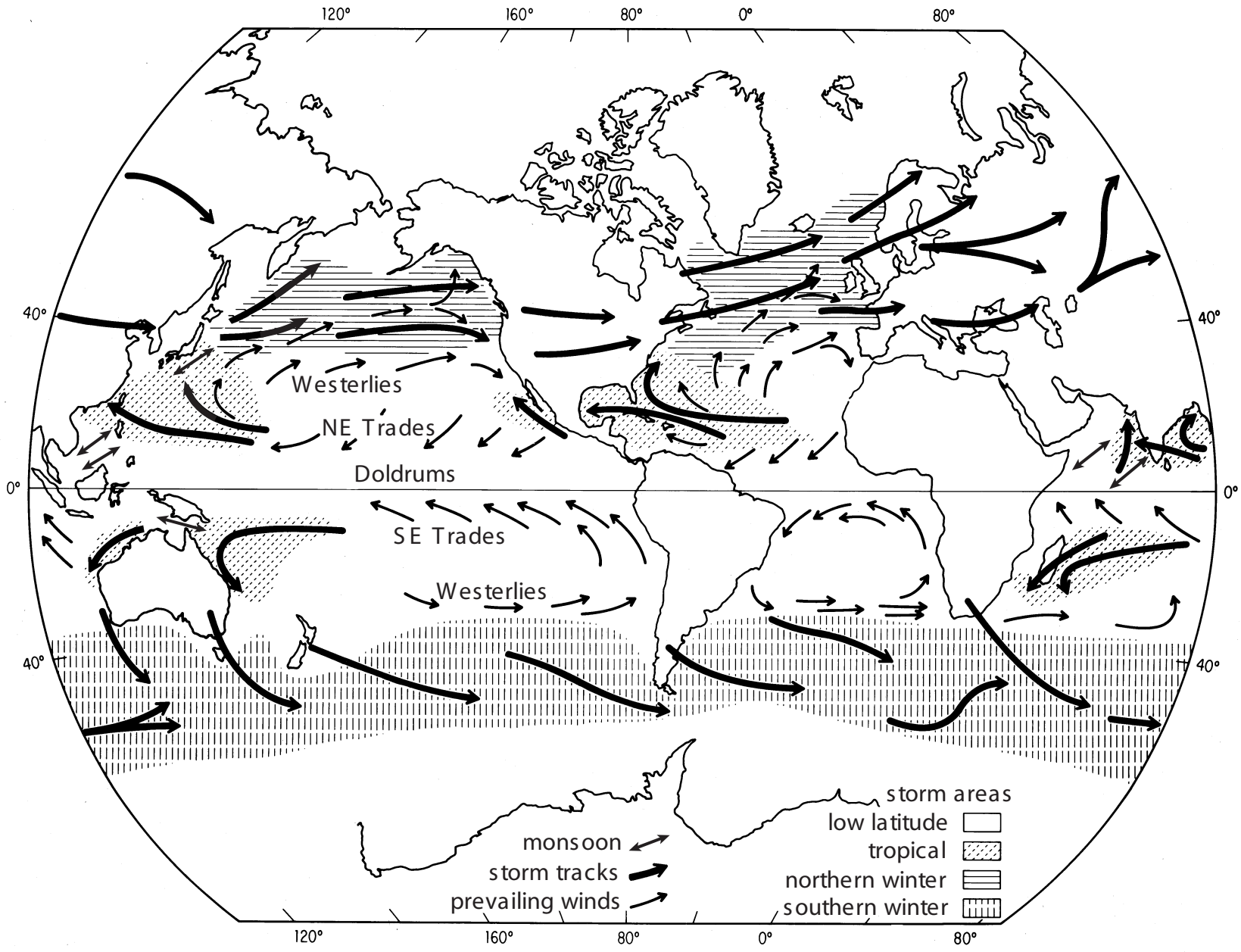

Figure 1. Prevailing winds and storm tracks for the world oceans.

Long, low frequency swell is typically absent from leeward coasts. Rather they are subject to periodic, intense sea waves from the poleward and easterly traveling storm fronts. The tracks for tropical (summer/fall) storms for the middle Atlantic seaboard of the United States essentially follow the Gulf Stream, while the extratropical (winter/spring) tracks take a more easterly course. In midlatitudes the tracks are channeled between the coast and the perimeter of the Bermuda high. This channel is sometimes known as the Atlantic seaboard cyclone track (e.g., Klein and Winston, 1958). In the vicinity of Cape Hatteras, the highest waves from both extra- and tropical storms are from the northeast. The storm tracks are offshore and generally parallel the coast, so that the counter-clockwise flowing winds in the northwest quadrant of the cyclone (winds blowing from the northeast) are the strongest and have the longest fetch (e.g., Dolan *et al.,* 1990). Thus prevailing waves along windward coasts and the strongest cyclonic sea waves along leeward coasts both have net components towards the equator. As a consequence, there is a world-wide tendency in midlatitudes (20°–45°) for the net wave-induced littoral transport of sand to be towards the equator.

A three meter-high surface wave at sea transmits 100 kW for every meter of wave crest, or 100 megawatts/km. Since wave energy increases as the square of wave height, most coastal energy is from high waves during storms, particularly storms of long duration. For example, the northeast storm of March 1989 along the Outer Banks of North Carolina had average deep water wave heights of 3 m (Dolan *et al.,* 1990). These were not unusually high waves, but they persisted for 115 hours and had a power expenditure of 11,500 kilowatt hours per meter of coastline (kWh/m). The average energy-flux of waves on the Outer Banks is about 2kW/m, which sums to a yearly total of 17,500 kWh/m (Inman and Dolan,

1989). Thus this one storm had a power expenditure (and sand transport potential) equivalent to 66% of that for the average year.

Data of instrumented buoys and light vessels in the North Atlantic and North Pacific all show that wave heights have increased significantly and continuously during the past 25 years (e.g., Graham and Diaz, 2001). The North Atlantic data show that the average annual (root-mean square) wave height has increased about 2% per year between 1962 and 1986. Over the 24 year period 1962-1986 the range in average annual *significant wave* ($\sqrt{2}$ times root-mean square) height at Seven Stones Light Vessel off Lands End, southwest England, ranged from 2.2 m to 2.9 m with an annual increase of 3 cm/yr. The "50-year return value" ranged from 12 m to 18 m with an increase of 20 cm/yr (Carter and Draper, 1998). Data from six buoys between latitude 34^{o} to 56^{o} in the eastern North Pacific show similar increasing trends over the period 1975 To 1999. The annual average significant wave height increased on average about 2 cm/yr, ranging for the six buoys from 0.4 cm - 4.2 cm/yr (Allen and Komar, 2000).

A preliminary estimate of global wave energy can be attempted from the data obtained from instrumented buoys and weather stations in the North Pacific and North Atlantic. The measurements for the eastern North Pacific cover the 25 year time interval from 1975-1999 (Allen and Komar, 2000). Over this period, the average annual (root-mean square) wave height increased progressively from about 1.6 m to 1.9 m, generating a landward wave energy flux that ranged for these average waves from about 93×10^6 kW to 131×10^6 kW over the same period. Thus the wave height increased about 20% while the corresponding energy flux increased about 40%. Similar wave conditions and wave-height increases over about the same period were observed for the eastern North Atlantic

Ocean (Carter and Draper, 1998). If it is assumed that the energy partitioning between periods of calm and storm results in an energy flux twice that estimated from the average annual wave height (i.e., the significant wave assumption), then the total annual energy flux over the 25 year period in the North Pacific becomes about 190 and 260 x 10^6 kW with an average for the period of about 230 x 10^6 kW for this 30-60^o latitude portion of the windward coast of North America.

When the energy flux of 260 x 10^6 kW for the North Pacific Ocean is extrapolated to the world oceans, the total wave energy flux to the global coastline becomes 2.5 x 10^9 kW (Table 2, footnote a). This is in agreement with earlier estimates (e.g., Inman, 1973) and gives an average energy flux of 5.7 kW/m to the 440,000 km of world coastline.

What is known about wave climate intensity suggests that windward coasts of oceans in the northern hemisphere are in phase with each other during El Niño and La Niña events and out of phase with lee coasts. In terms of decadal climate patterns, that are alternately El Niño or La Niña dominated, the prevailing wind stress and swell directions in the northern and southern hemisphere appear to be out of phase (Trenberth and Hurrell, 1994; Chao *et al.,* 2000). For example, during the La Niña dominated climate of the third-quarter of the 20th century, waves from the southern ocean appeared as "southern swell" along the California coast. Southern swell was absent from the California coast during the previous quarter of the century and again disappeared during the last quarter century (Inman and Jenkins, 1997). This is because of a global realignment in predominant storm tracks with changes in the phase of PDO, where El Niño storm tracks tend to be more zonal than those of La Niña storms. Consequently the long waves of El Niño storms do not generally propagate out of the hemisphere in which they were

Table 2. Estimates of the flux of mechanical energy in the shallow waters of the world in units of 10^9 kW.

Wind-generated waves breaking against the shoreline [a]	2.5
Tidal currents due to surface tides on shelves and in shallow seas [b]	2.2
Currents due to internal waves and tides over shelves [c]	0.5
Large scale ocean currents in shallow seas [b]	0.2
All other sources	0.1
TOTAL	5.5

a Assuming the average energy-flux for the six instrumented NOAA buoys in the eastern North Pacific (Allen and Komar, 2000), proportioned over 30^o-60^o north latitude, is 230 x 10^6 kW (see text) and that for the 0^o-30^o portion of the eastern North Pacific is one-half, and that for the leeward ocean coasts is one third that of the windward coasts, giving a total for the coasts bordering the North Pacific Ocean of 460 x 10^6 kW. The global flux is assumed to be equivalent to that from five and one-half oceans like the North Pacific Ocean (i.e., North and South Pacific Oceans, North and South Atlantic Oceans, Indian Ocean, and one-half "ocean" equivalence for all marginal seas).

b Inman and Brush (1973).

c Conservative estimate from Wunsch and Hendry (1972).

generated. Conversely, the frontal circulation of La Niña storms is more meridional, generating waves that traverse latitude. Therefore, the northern hemisphere beaches are usually affected by southern hemisphere swells only when the southern hemisphere is in a La Niña dominated climate pattern.

Studies of windfields and pressure gradients indicate that the increase in wave heights in the eastern North Atlantic during the last quarter of the 20th century resulted from intensification of the pressure gradients between the Iceland low and the Azores high which could be related to climate change associated with the North Atlantic Oscillation (NAO) (Kushnir *et al.,* 1997). It is likely that some of the increase in wave intensity in the eastern North Pacific Ocean was associated with the Pacific Decadal Oscillation and increased sea surface temperatures during the last quarter of the century. However it is unclear what portion of these increased wave heights in the North Atlantic and North Pacific oceans are also associated with global warming (Graham and Diaz, 2001). If the increases are mainly due to decadal oscillations, they suggest that decadal climate lead to ±30% changes in wave climate. (see entry on *Climate Patterns in the Coastal Zone*).

Tsunamis

The most impressive waves in the sea are those generated by submarine earthquakes, landslides, and volcanic explosions (e.g., Van Dorn, 1987). These waves, called *tsunamis*, are well known because of the loss of life and great damage to coastal structures associated with their passage. Of the many types of surface waves, tsunamis contain the highest instantaneous power surges. They are reported to have caused runup to heights as great as 50 m above sea level in modern times and to greater heights in ancient times. The explosion and collapse of the volcanic island of Thera (Santorini) about 1400 B.C. is thought to have

caused a tsunami about 11 m high at Crete (Yokoyama, 1978) that may have ended Minoan maritime supremacy. The largest, well-documented tsunami was associated with the explosion and collapse of Krakatoa volcano in Sunda Strait between the Indonesian Islands of Java and Sumatra in August 1883. The energy of the explosion is estimated to have been 2×10^{18} J (500 megatons of TNT) and it ejected 18 km^3 of material into the atmosphere (e.g., Simkin and Fiske, 1983). The resulting tsunami was estimated to be nearly 40 m in height; it drowned 36,000 people and destroyed 5,000 ships. One ship, the *Berouw* was carried 2 km inland on Sumatra where it remains today. The tsunami was observed on tide gages throughout the world, and dust from the explosion covered the entire world causing brilliant sunsets for many years.

Detectable tsunamis have occurred about once a year. However, truly large tsunamis with energy content as high as 5×10^{15} J occur only about five times per century. Averaged over long periods, tsunamis would generate an energy flux of about 1×10^5 kW. Thus, because of their relative infrequency, these catastrophic waves contribute little to the world-wide budget of power.

Tides

The gravitational forces of moon and sun provide the driving forces for the ocean tides, with the moon's tide generating force being about twice that of the sun. The main lunar (semidiurnal, M_2) tide with a period of 12.42 hour is the principal world tide; however, the interaction between lunar and solar forces provides a variety of tide-generating constituents. Locally, tidal amplitudes are determined in part by the interactions of the propagating oceanic tidal bulge with the shape of the ocean basin, favoring oscillations that are harmonics of the tidal forcing and the basin dimensions. The dominant tidal oscillations are usually

referred to as *semidiurnal* (twice daily), *diurnal* (once daily), and *mixed* tides that are combinations of the two, such as those along the Pacific coast of the Americas.

The ocean surface tides, having wavelengths that are very long compared with the depth of the ocean, produce some motion even in the deepest water. However, this motion is usually only a few centimeters per second so that the energy dissipation by tides against the deep sea bottom is slight. The principal tidal dissipation results from the flow of strong tidal currents in shallow areas, such as the Bering Sea and the Argentine shelf. One of the more impressive tidal coastlines occurs in Argentina. The tidal wave travels eastward through Drake Passage and then northward where it shoals over the broad Argentine shelf, attaining spring ranges of nearly 15 m at Rio Gallegos. From the southeastern tip of Tierra del Fuego to Bahia Blanca, a distance of 2800 km, the tidal range is mostly in excess of 6 m.

"Tides are unique among natural physical processes in that one can predict their motions well into the future with acceptable accuracy without learning anything about their physical mechanism" (Cartwright, 1977). Their prediction from tide gauge records has been possible since Darwin formulated the rules of harmonic tide prediction in 1883. But, prediction from harmonic constituents can be in error when changing wind fields and warm water associated with El Niño events raise and lower sea level by 30 cm and more.

The energy dissipated by various kinds of tidal currents against the shallow sea bottom is one of the major factors that causes the rotational deceleration of the earth. Much of our present knowledge of this dissipation results from investigations by geophysicists into the possible causes of the deceleration in the earth's rotation (Jeffreys, 1920, 1970; Munk and MacDonald, 1960). Tidal dissipation

causes a lag in the tidal bulge of the Earth relative to the rotation of the Earth-moon system. This bulge exerts a torque that results in a decrease in both the Earth's rotation rate and in the lunar orbital velocity.

From telescopic observations of sun and moon over the previous two and one-half centuries, Spencer Jones (Munk and MacDonald, 1960) determined that the moon's deceleration was 22.4 arcsec/century^2. This deceleration would be associated with an energy dissipation in the atmosphere, oceans, and solid earth of about 2.7 x 10^9 kW. More recently, measurements of the change in the moon's semimajor axis using laser ranging techniques show that the frictional energy dissipation due to the M_2 tides is 3.1 x 10^9 kW, giving a dissipation rate due to the solar and lunar tides of about 4.0 x 10^9 kW (e.g., Dickey *et al.,* 1994). The allocation by process for these revised dissipations of tidal energy is not yet understood. The best estimates for the lunar tidal dissipation in shallow seas is that of Miller (1966). He used the method of energy flux into shallow seas, rather than the less accurate method of summing the energy loss due to frictional drag on unit area of the bottom. His value of 1.7 x 10^9 kW for lunar tidal energy dissipation, when corrected for the solar tidal flux, gives a total energy dissipation for shallow seas of 2.2 × 10^9 kW (Table 2).

Internal waves

Internal waves are water oscillations that occur within the various density layers beneath the ocean surface. It appears that far more energy is transformed into internal (baroclinic) waves than was previously thought. The vertically-integrated energy over the deep sea is typically about 4 × 10^{-3} J/m^2 (e.g., Garrett and Munk, 1979). Mechanisms generating internal waves include direct coupling between ocean surface waves and the density layers beneath the surface, scattering

due to sea floor roughness (Cox and Sandstrom, 1962), and generation by impingement of deep sea tides on the slopes of the continental shelves and submarine canyons (Rattray *et al.*, 1969).

Cox and Sandstrom (1962) found that internal waves were coupled to surface waves and estimate that the rate of conversion of tidal energy into internal wave energy in the Atlantic Ocean is roughly between 6 and 69 percent of the power of the surface tide. From this, Munk and MacDonald (1960) estimate that the conversion of energy from surface to internal modes on a global scale may be about 1.5×10^9 kW. Most internal wave energy is contained in the areas of deep ocean, but some of the energy travels into shallow water and is dissipated against the sea bottom. Winant (1974) estimated that the dissipation due to runup of breaking internal waves and surges on the shelves of the world may range between 2×10^5 and 2×10^7 kW.

Wunsch and Hendry (1972) measured currents from an array placed on the continental slope off Long Island, New York, and concluded that the onshore energy flux of internal waves was 6 W/m. Assuming this to be a typical value, they estimated that the world-wide onshore flux of energy would be about 0.7×10^9 kW. A value of about 0.5×10^9 kW for the energy dissipation by internal waves over the world's shelves appears to be a reasonable estimate (Table 2).

Ocean currents, large and small

The kinetic energy associated with large-scale ocean currents is very large compared with the energy in surface waves and tidal currents. Stommel (1958) estimates that the average kinetic energy of currents in the North Atlantic Ocean is about 2×10^{17} J. Flows such as the equatorial and Antarctic Circumpolar currents transport water at rates of 50 to 200 Sverdrup (million cubic meter per second).

Even the relatively small California current transports about 12 Sverdrup, a discharge that is greater than that of all the rivers and streams in the world. In addition to the surface currents, the world ocean has a surprisingly large circulation of deep and bottom water estimated to be 50 Sverdrup (e.g., Schmitz, 1995).

Intense western boundary currents, such as the Gulf Stream, develop instabilities with horizontal waves or meanders. These meanders form large loops that may close or pinch-off, forming circular eddies or rings. These *mesoscale eddies* are typically 100 km and more in diameter, and since they are in cycloidal balance, conservation of angular momentum causes them to persist for many months to a year or so, as they move thousands of km away from the main current. Eddies that breakoff from the poleward side of the currents have warm-cores and cyclonic rotation, whereas those shed from the equatorial side have cold-cores and anticyclonic motion (e.g., Gill, 1982). The details of the global distribution of the energy in mesoscale eddies is not well-known except for satellite observations of western boundary currents. The effects of mesoscale eddies on the continental shelves is poorly understood, although it is known that shelf eddies are associated with wind changes and with coastal promontories (e.g., Davis, 1985).

While the flow of major ocean currents is predominantly in deep water, their boundaries overlap the continental shelves, and the currents dissipate some of their energy against the shallow sea bottoms. For example, the Guiana (North Brazil) Current, with a volume discharge of about 29 Sverdrup, flows with velocities up to 1 m/s over the 0.5×10^6 km^2 of shelf off the coastlines of the Guianas and northern Brazil (e.g., Fratantoni, *et al.,* 1995). The Falkland Current flows with velocities of 25 cm/s to 50 cm/s across the 1×10^6 km^2 of shallow shelf off Patagonia. If the

Guiana Current averages 50 cm/s and the Falkland Current averages 25 cm/s, they would dissipate energy at the rate of 0.13×10^9 and 0.03×10^9 kW, respectively. Therefore it seems likely that the world-wide dissipation of energy from the flow of ocean currents in shallow water may be about 0.2×10^9 kW (Table 2).

Other sources

In addition to generating the ocean's waves, atmospheric winds and pressures have important local effects near shore. Pressure fronts generate shelf seiche, and the combination of pressure and wind stress on the water's surface produces local anomalies in sea level that induce circulation of water over the shelf and in submarine canyons. Shelf seiche up to a meter in height or more are common along the Argentine coast (Inman *et al.,* 1962), while the sea level anomalies associated with storm surges may exceed four meters for severe storms (Pugh, 1987). Also, winds blowing over the coastal zone dissipate energy on beach and sand dunes. On a world-wide basis, this dissipation may be about 1×10^7 kW, and because of the prevalence of sea breeze and other onshore winds, results in a net inland transport of beach sand.

From the foregoing discussion, it appears that the total flux of mechanical energy in the shallow waters of the world is about 5.5×10^9 kW (Table 2). Dissipation and work by one process or another occurs over the entire shelf. The wind-generated surface waves expend their energy primarily nearshore, especially in the breaker zone, while tidal and other ocean currents and internal waves dissipate energy mostly over the outer portions of the shelf. Internal waves, edge waves, shelf seiche, and local winds may produce water motion over the continental shelf and submarine canyons.

Budget of sediment

The shoreline is the junction of the realms of terrestrial erosion and marine deposition. Thus it is the unique singularity between air, land, and sea, and the shoreline is the critical datum for dynamical geology. In 1955 James Gilluly calculated that sediment is now being carried across this boundary at a rate great enough, in the absence of mountain building, to "erase all the topography above sea level in less than 10 million years . . . ," a very short time on the geological time scale. Thus the supply of sediment associated with runoff from the continents is large, and it has increased during the past 10 million years due to climate variability, especially during the Pleistocene and more recently due to human intervention. The principal sources of beach and nearshore sediments are the rivers that bring large quantities of sand directly to the ocean, the sea cliffs of unconsolidated material that are eroded by waves, and material of biological origin such as shells, coral fragments, and skeletons of other small marine organisms (Figure 2). Also, waves may transport onshore relict sands that were deposited along the inner shelf during lower stands of the sea (e.g., Inman and Dolan, 1989).

Sediment yield increases with the relief of the drainage basin and with decrease in basin size, factors that enhance the sediment flux of small rivers along mountainous coasts (Inman and Jenkins, 1999). Climate, rainfall, and type of geologic formation are also well known factors in determining sediment yield. Maximum yield occurs for basins in temperate climates that receive an annual rainfall of about 25-50 cm, and decreases for precipitation rates either above or below this maximum (Langbein and Schumm, 1958). In arid climates, the occasional flash floods transport large volumes of sand (Figure 3).

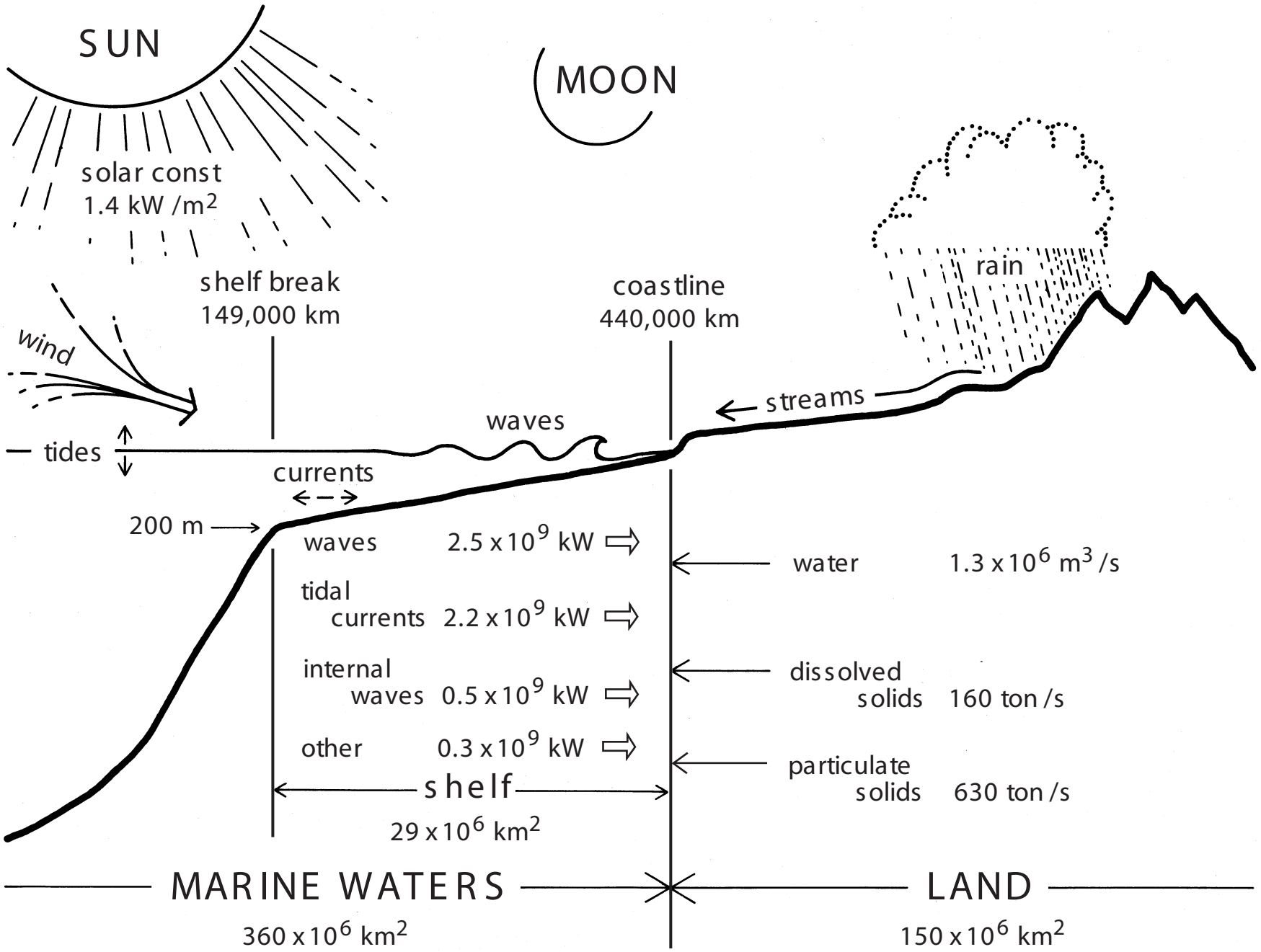

Figure 2. Schematic diagram of budget of energy dissipation in nearshore waters, and the runoff of water and sediment from the land [after Inman, 1973]. Data from Tables 1-3.

Figure 3. Streams carry erosion products from the land to the sea; El Moreno, Gulf of California, Mexico.

Man's intervention in natural processes is accelerating erosion rates, perhaps by a factor of about two on a global scale (Milliman and Syvitski, 1992; Vitousek *et al.*, 1997). Significant anthropogenic effects began as early as 9000 years ago with deforestation and the spread of agriculture from the "Fertile Crescent" (e.g., Heun *et al.,* 1997). Man's intervention has accelerated in this century with increased deforestation, expansion of mechanized agriculture, proliferation of dams (Meade, 1996), and since World War II with extensive urbanization of coastal lands particularly in central and southern California. Urbanization decreases erosion locally, but accelerates streambed erosion in response to the greater frequency and magnitude of peak streamflow due to runoff from impervious urban surfaces (e.g., Trimble, 1997).

The effects of changing climate and sea level rise have been studied extensively on a glacial/interglacial time scale (e.g., Hay, 1994) and during the Holocene on a millennial scale (e.g., Bond *et al.,* 1997). The effect of decadal scale climate changes on the sediment flux of the 20 largest streams entering the Pacific Ocean along the central and southern California coast was studied by Inman and Jenkins (1999). The annual streamflow ranged from zero during dry years to a maximum of 1.1×10^9 m^3/yr for the Santa Clara River in 1969 with an associated suspended sediment flux of 46×10^6 ton. Trend analyses showed that El Niño/Southern Oscillation (ENSO) induced climate changes recur on a multidecadal time scale in general agreement with the Pacific/North American (PNA) climate pattern: a dry climate extending from 1944 to about 1968 and a wet climate extending from about 1969 to 1998. The dry period is characterized by consistently low annual river sediment flux. The wet period had a mean annual suspended sediment flux about 5 times greater, caused by strong El Niño events

that produce floods with an average recurrence of about 5 years. The sediment flux of the rivers during the three major flood years averaged 27 times greater than the annual flux during the previous dry climate (see entry *Climate Patterns in the Coastal Zone*).

The effects of climate change are superimposed on erodibility associated with basin geology. The sediment yield of the faulted, overturned Cenozoic sediments of the Transverse Ranges of California is many times greater than that of the Coast Ranges and Peninsular Ranges. Thus the abrupt transition from dry to wet climate in 1969 brought a suspended sediment flux of 100 million tons to the ocean edge of the Santa Barbara Channel from the rivers of the Transverse Range, an amount greater than their total flux during the preceding 25 year dry period. These alternating dry to wet decadal scale changes in climate are natural cycles that have profound effects on fluvial morphology, engineering structures, and the supply of sediment.

Cliff erosion probably does not account for more than about five percent of the material on most beaches. Wave erosion of rocky coasts is usually slow, even where the rocks are relatively soft shales. On the other hand, erosion rates greater than 1 m/yr are not uncommon in unconsolidated sea cliffs and dunes as found on trailing-edge coasts such as the east coast of the United States.

Following initial deposition at the mouths of streams entering the ocean, much of the sand-size portion of terrestrial sediments is carried along the coast by waves and wave-induced longshore currents. The sand carried by these longshore currents may be intercepted by submarine canyons that cut into the continental shelf and divert the sand into deeper water offshore. Since submarine canyons occur along most coasts, except those bordered by shallow seas, they probably

account for most of the sediment lost into deep water from the nearshore. Notable among the major sediment transporting submarine canyons of the world are Cap Breton Submarine Canyon on the Atlantic coast of France; Cayar and Trou Sans Fond, and Congo Canyons on the Atlantic coast of Africa; the Indus and the Ganges Submarine Canyons in the Indian Ocean; and the Monterey Submarine Canyon on the Pacific Coast of North America. Observations by H. W. Menard (1960) suggest that most of the deep sediments on the abyssal plains along a 400 km section of the California coastline are derived from two submarine canyons; the Delgada Submarine Canyon in Northern California and Monterey Submarine Canyon in central California. These canyons cut the continental shelf almost to the shoreline, and consequently they trap and divert an estimated sediment volume of about 1 x 10^6 m^3/yr (see entry on *Littoral Cells*).

Traditionally, geologists have estimated long term erosion and deposition rates from the amount of material deposited during geological time. Such estimates give erosion rates varying from about 1 to 4 cm per thousand years (cm/ky) for drainage basins of moderate relief to as high as 21 to 100 cm/ky for the Himalaya Mountains (e.g., Gilluly, 1955). Assessment of the volume of sedimentary material on the continental United States and in its adjacent sea floors indicates that the average erosion rate of the United States during the past 600 million years was 3 to 6 cm/ky (Gilluly *et al.*, 1970).

An increasing number of measurements of river discharge have provided an independent estimate of contemporary erosion rates of the land. The importance of large rivers in transporting the denudation products of the continents to the sea has been known since Lyell (1873) described the flux of sediment into the Bay of Bengal from the Ganges and Brahmaputra Rivers. Since then the contributions

from large rivers have been updated and summarized in many studies (e.g., Garrels and Mackenzie, 1971; Inman and Brush, 1973; Meade, 1996) with estimates of the total flux of particulate solids to the ocean of about 16 x 10^9 ton/yr. The importance of small rivers to the global budget of sediment was first documented by Milliman and Syvitski (1992). They showed that small rivers (drainage basin < 10,000 km^2) cover only 20% of the land area but their large number results in their collectively contributing much more sediment than previously estimated, increasing the total flux of particulate solids to about 20 x 10^9 ton/yr (630 ton/s) by streams and rivers (Table 3).

Balance of the budgets of power and sediment

The global flux of erosion products from the land to the sea include 160 ton/s dissolved solids and 630 ton/s particulate solids (Table 3). The dissolved solids are incorporated into the 1.3 x 10^6 m^3/s flow of "fresh" water as added mass. Most of the particulate solids carried by streamflow are fine silt and clay size material that move as suspended load and washload. The remaining solids are sand and coarser material that move mostly as bed and suspended load. Once the stream discharges into the sea, there are significant differences in the transport paths of the suspended and bedload sediment. Most of the fine suspended sediment moves with the river water and flows out over the sea as a spreading turbid plume, and the sediment, which is subject to flocculation and ingestion by organisms, is eventually deposited in deeper water. The coarser bedload material remains near the river mouth as a submerged sand delta and is later transported along the shore by waves and currents to nourish the downcoast beaches. The few reliable measurements of bedload indicate that it is ca. $\leq$10% of the total load in large

Table 3. Estimate of the natural runoff of fresh water and solids from the continents into the oceans and coastal waters of the world.

Discharge of water into the oceans from all rivers [a]	1.3×10^6 m^3/s
Flux of dissolved solids [b]	160 ton/s
Flux of particulate solids [b]	630 ton/s
Flux of particulate solids from sea cliff erosion [c]	> 2 ton/s
Flux of eolian particulate solids [d]	14 ton/s
Average erosion rate of land [b]	6 cm per 10^3 years

a Average value (1.1×10^6 m^3/s) from Turekian (1971), Alekin and Brazhnikov (1961) and Holeman (1968) updated in proportion to increase in particulate solids from 530 ton/s to 630 ton/s.

b Assuming that continental rock of density 2.7 ton/m^3 erodes to form 20% dissolved load and 80% solid particulate load. Assuming flux of particulate solids is 630 ton/s (Milliman and Syvitski, 1992).

c Emery and Milliman, 1978.

d windblown dust, volcanic and forest fire ash (Prospero and Carlson, 1981; Rea, 1994; Prospero *et al.*, 2002).

rivers but, in smaller, mountainous streams, may be considerably more (Richards, 1982; Inman and Jenkins, 1999).

It is of interest to compare the global fluxes of energy and sediments into the coastal waters of the world (Figure 2). Since energy provides the capacity for doing work, the flux of energy associated with waves and currents is a measure of their potential to transport sediment. About one-half (2.9×10^9 kW) of the total flux of mechanical energy is associated with currents of various types, internal waves, and turbulence, and this flux acts primarily upon the fine particulate solids that flow out over the ocean surface. The remaining energy (2.5×10^9 kW) is from ocean surface waves and works primarily on sand size solids that are deposited in shallow water. About 85% (535 ton/s) of the particulate solids are fine material, while about 15% (95 ton/s) are sand and coarser.

Waves move sand on, off, and along the shore. Once an equilibrium beach profile is established, the principal transport is along the coast. Theory and field measurements show that the littoral transport rate of sand along a beach is proportional to the energy flux of the incident waves, where the proportionality is a function of the direction of wave approach relative to the shoreline. If 10% of the world's estimated annual wave power at the coast (0.25×10^9 kW) is available for transporting sediment (i.e. the wave breaker angle is about 5°), the waves have the potential to transport the entire sand size load of solids in the world's streams (95 ton/s) a distance of 750 km along the coast each year. Thus, even under the inefficient coupling that exists in nature, it is apparent that the potential for sediment transport in nearshore waters is large.

Douglas L. Inman and Scott A. Jenkins

Bibliography

Alekin, O. A., and Brazhnikova, L. V., 1961. The discharge of soluble matter from dry land of the earth. *Gidrokhim. Materialy,* **32**, 12-24.

Allen, J., and Komar, P., 2000. Are ocean wave heights increasing in the eastern North Pacific. *EOS*, **81**, 561-7.

Bond, G., Showers, W., Cheseby, M., Lotti, R., Almasi, P., deMenocal, P., Priore, P., Cullen, H., Hajds, I., and Bonani, G., 1997. A pervasive millennial-scale cycle in North Atlantic Holocene and glacial climates. *Science*, **278**, 1257-66.

Carter, D. J. T., and Draper, L., 1988. Has the north-east Atlantic become rougher? *Nature*, **332**, 494.

Cartwright, D. E., 1977. Oceanic tides. *Reports on Progress in Physics*, **40**, 665-708.

Chao, Y., Ghil, M. and McWilliams, J. C., 2000. Pacific interdecadal variability in this century's sea surface temperatures. *Geophysical Res. Letters*, **27**, 2261-4.

Cox, C., and Sandstrom, H., 1962. Coupling of internal and surface waves in water of variable depth. *Jour. Oceanographical Society of Japan*, 20th Anniversary Volume, 499-513.

Davis, R. E., 1985. Drifter observations of coastal surface currents during CODE: The method and descriptive view. *Jour. Geophysical Res.*, **90**, 4741-55.

Dickey, J. O., and 11 others, 1994. Lunar laser ranging: A continuing legacy of the Apollo Program. *Science*, **265**, 482-90.

Dolan, R., Inman, D. L., and Hayden, B. P., 1990. The Atlantic coast storm of March 1989. *Jour. Coastal Research*, **6**, 721-5.

Emery, K. O., and Milliman, J. D., 1978. Suspended matter in surface waters: influence of river discharge and upwelling. *Sedimentology*, **25**, 125-40.

Fratantoni, D. M., Johns, W. E. and Townsend, T. L., 1995. Rings of the North Brazil Current: Their structure and behavior inferred from observations and a numerical simulation. *Jour. Geophysical Research*, **100**, 10-633-54.

Garrels, R. M., and MacKenzie, F. T., 1971. *Evolution of Sedimentary Rocks*. New York: W. W. Norton & Co.

Garrett, C., and Munk, W., 1979. Internal waves in the ocean. In Van Dyke, M., Wehausen, J. V., and Lumley, J. L., (eds), *Annual Review of Fluid Mechanics, Volume 11*. Palo Alto: Annual Reviews Inc., pp. 339-69.

Gill, A. E., 1982. *Atmosphere-Ocean Dynamics*. Orlando: Academic Press.

Gilluly, J., 1955. Geologic contrasts between continents and ocean basins. In Poldervaart, A., (ed), *Crust of the Earth*. Geological Society America, Special Paper 62, pp. 7-18.

Gilluly, J., Reed, J. C. Jr., and Cady, W. M., 1970. Sedimentary volumes and their significance. *Geological Soc. Amer. Bull.*, **81**, 353.

Graham, N. E. and Diaz, H. F., 2001. Evidence for intensification of North Pacific winter cyclones since 1948. *Bull. Amer. Meteor. Soc.*, **82**, 1869-93.

Hay, W. W., 1994. Pleistocene-Holocene fluxes are not the Earth's norm. In *Material Fluxes on the Surface of the Earth*. Washington, D. C.: National Academy Press, pp. 15-24.

Heun, M., Schäfer-Pregl, R., Klawan, D., Castagna, R., Accerbi, M., Borghi, B., and Salamini, F., 1997. Site of einkorn wheat domestication identified by DNA fingerprinting. *Science*, **278**, 1312-4.

Holeman, J. N., 1968. The sediment yield of major rivers of the world. *Water Resources Research*, **4**, 737-41.

Inman, D. L., Munk, W. H., and Balay, M., 1962. Spectra of low frequency ocean waves along the Argentine Shelf. *Deep-Sea Research*, **8**, 155-64.

Inman, D. L., and Nordstrom, C. E., 1971. On the tectonic and morphologic classification of coasts. *Jour. of Geology*, **79**, 1-21.

Inman, D. L., 1973. Shore processes. In Vetter, R. C. (ed) *Oceanography: The Last Frontier*. New York: Basic Books, Inc., pp. 317-38.

Inman, D. L., and Brush, B. M., 1973. The coastal challenge. *Science*, **181**, 20-32.

Inman, D. L., and Dolan, R., 1989. The Outer Banks of North Carolina: Budget of sediment and inlet dynamics along a migrating barrier system. *Jour. Coastal Res.*, **5**, 193-237.

Inman, D. L., and Jenkins, S. A., 1997. Changing wave climate and littoral drift along the California coast. p. 538-549 in O. T. Magoon et al., eds., *California and the World Ocean '97*, ASCE, Reston, VA, 1756 pp.

Inman, D. L., and Jenkins, S. A., 1999. Climate change and the episodicity of sediment flux of small California rivers. *Jour. Geology*, **107**, 251-70.

Jeffreys, H., 1920. Tidal friction in shallow seas. *Phil. Trans. Royal Society*, **221**, 239-64.

Jeffreys, H., 1970. *The Earth; Its Origin, History and Physical Constitution*. Cambridge: University Press.

Klein, W. H., and Winston, J. S., 1958. Geographical frequency of troughs and ridges on mean 700 mb charts. *Monthly Weather Rev.*, **86**, 344-58.

Kushnir, Y., Cardone, V. J., Greenwood, J. G., and Cane, M. A., 1997. The recent increase in North Atlantic wave heights. *Jour. Climate*, **10**, 2107-13.

Langbein, W. B., and Schumm, S. A., 1958. Yield of sediment in relation to mean annual precipitation. *Trans. Am. Geophys. Union*, **39**, 1076-84.

Lyell, C., 1873. *Principles of Geology*, Volume 1. New York: D. Appleton and Company.

Malkus, J. S., 1962. Interchange of properties between sea and air: Large-scale interactions. In Hill, M. N., (ed), *The Sea, v. 1, Ideas and Observations*. NewYork: Interscience Publ., pp. 88-294.

Meade, R. H., 1996. River-sediment inputs to major deltas. In Milliman, J. D., and Haq, B. U., (eds), *Sea-level rise and coastal subsidence*. Dordrecht: Kluwer, pp. 63-85.

Menard, H. W., 1960. Possible pre-Pleistocene deep-sea fans off central California. *Geological Society America*, **71**, 1271-8.

Miller, G. R., 1966. The flux of tidal energy out of the deep oceans. *Jour. Geophysical Res.*, **71**, 2785-9.

Milliman, J. D., and Syvitski, J. P. M., 1992. Geomorphic/tectonic control of sediment discharge to the ocean: The importance of small mountainous rivers. *Jour. Geology*, **100**, 525-44.

Munk, W. H., and MacDonald, G. J. F., 1960. *The rotation of the Earth; a geophysical discussion*. London: Cambridge University Press.

Newell, R. E., Newell, N. E., Zhu, Y., and Scott, C., 1992. Tropospheric rivers? - A pilot study. *Geophysical Res. Letters*, **12**, 2401-4.

Pollack, H. N., Hurter, S. J., and Johnson, J. R., 1993. Heat flow from the earth's interior: Analysis of global data set. *Reviews of Geophysics*, **31**, 267-80.

Prospero, J. M., and Carlson, T. N., 1981. Saharan air outbreaks over the tropical North Atlantic. *Pure and Applied Geophysics*, **119**, 677-91.

Prospero, J. M., Ginoux, P., Torres, O., Nicholson, S. E., and Gill, T. E., 2002. Environmental characterization of global sources of atmospheric soil dust identified with the Nimbus 7 Total Ozone Mapping Spectrometer (TOMS) absorbing aerosol product. *Reviews of Geophysics*, **40**, 31 pp.

Pugh, D. T., 1987. *Tides, Surges and Mean Sea-Level*. New York: John Wiley & Son.

Rasmussen, D., 1996. State Mussel Watch Program, 1993-1995, Data Report 96-2WQ. Sacramento: State Water Resources Control Board, California Environmental Protection Agency.

Rattray, M., Dworski, J. G., and Kovala, P. E., 1969. Generation of long internal waves at the continental slope. *Deep-Sea Research*, **16**, 179-96.

Rea, D. K., 1994. The paleoclimatic record provided by eolian deposition in the deep sea: The geologic history of wind. *Rev. Geophysics*, **32**, 159-95.

Richards, K., 1982. *Rivers, Form and Processes in Alluvial Channels*. London: Methuen.

Schmitz, W. J. Jr., 1995. On the interbasin-scale thermohaline circulation. *Rev. Geophysics*, **33**, 151-73.

Shepard, F. P., 1963. *Submarine Geology* (2nd ed), New York: Harper & Row.

Simkin, T., and Fiske, R. S., 1983. *Krakatau 1883: The Volcanic Eruption and Its Effects*. Washington, D. C.: Smithsonian Inst. Press.

Stommel, H., 1958. *The Gulf Stream, a Physical and Dynamical Description*. Berkeley: University of California Press.

Trenberth, K. E., and Hurrell, J. W., 1994. Decadal atmosphere-ocean variations in the Pacific. *Clim. Dyn.*, **9**, 303-19.

Trimble, S. W., 1997. Contribution of stream channel erosion to sediment yield from an urbanizing watershed. *Science*, **278**, 1442-4.

Turekian, K. K., 1971. Rivers, tributaries, and estuaries. In Hood, D. W., (ed), *Impingement of Man on the Oceans*. New York: Wiley-Interscience, pp. 9-72.

UNEP, 1987. The state of the world environment. *United Nations Environmental Programme*, UNEP/GC.14/6, 76 pp.

Van Dorn, W. G., 1987. Tide gage response to tsunamis. Part II: Other oceans and smaller seas. *Jour. Physical Oceanogr.*, **17**, 1507-16.

Vitousek, P. M., Mooney, H. A., Lubchenco, J., and Melillo, M. M., 1997. Human domination of Earth's ecosystems. *Science*, **277**, 494-9.

Webster, P. J., 1994. The role of hydrological processes in ocean-atmosphere interactions. *Rev. Geophysics*, **32**, 427-76.

Winant, C. D., 1974. Internal surges in coastal waters. *Jour. Geophysical Res.*, **79**, 4523-6.

Wunsch, C., and Hendry, R., 1972. Array measurements of the bottom boundary layer and internal wave field on the continental slope. *Geophysical Fluid Dynamics*, **4**, 101-45.

Yokoyama, I., 1978. The tsunami caused by the prehistoric eruption of Thera. In Doumas, C., (ed), *Thera and the Aegean World*. London: pp. 277-283.

Cross-references

Accretion and Erosion Waves
Beach Processes
Climate Patterns in the Coastal Zone
Currents
Databases
Erosion Processes
Global Warming
History, Coastal Geomorphology
Human Impact on Coasts
Littoral Cells
Longshore Sediment Transport
Meteorologic Effects
Sediment Budget
Waves
Weathering Processes